Bispecific PSMA-617 / RM2 Heterodimer for Theranostics Applications in Prostate Cancer

Christos Liolios, *[1,2,6] Danai Bouziotis, [2] George Lambrinidis, [3] Martin Schaefer, [1] Wiebke Sihver,[4] Evangelia-Alexandra Salvanou, [2] Ulrike Bauder-Wuest, [1] Martina Benesova, [1] Klaus Kopka, [4,5] Antonios Kolokouris, [3] Penelope Bouziotis *[2]

[1] Division of Radiopharmaceutical Chemistry, German Cancer Research Centre (DKFZ), Im Neuenheimer Feld 280, 69120 Heidelberg, Germany

[2] Radiochemical studies Laboratory, INRASTES, N.C.S.R. "Demokritos", Agia Paraskevi Attikis, 15310 Athens, Greece

[3] Laboratory of Medicinal Chemistry, Section of Pharmaceutical Chemistry, Department of Pharmacy, National and Kapodistrian University of Athens (NKUA), Panepistimiopolis–Zografou, 15771 Athens, Greece

[4] Institute of Radiopharmaceutical Cancer Research, Helmholtz-Zentrum Dresden-Rossendorf (HZDR), Bautzner Landstraße 400, 01328 Dresden, Germany

[5] Faculty of Chemistry and Food Chemistry, School of Science, Technical University Dresden, Raum 413 Bergstr. 66, 01069, Dresden, Germany

[6] Institute of Pharmaceutical Research & Technology, 18th km of Marathonos Avenue, 153 51, Pallini, Attica, Greece

Corresponding authors:

Christos Liolios, liolios.xr@gmail.com

Penelope Bouziotis, bouzioti@rrp.demokritos.gr

Abstract

PSMA and GRPR protein receptors are upregulated during prostate cancer (PCa) progression, and thus they have both been used for diagnostic molecular imaging and therapy of the disease. To address tumor heterogeneity, we synthesized and evaluated the bispecific PSMA/GRPR ligand (**3**) with a 10 atom spacer between PSMA-617 (**1**) and the GRPR antagonist RM2 (**2**) generated with click chemistry and coupled with chelator DOTA, to enable radiolabelling. Ligand **3** was radiolabelled with ^{68}Ga, [^{68}Ga]Ga-**3** and ^{177}Lu, [^{177}Lu]Lu-**3**. [^{68}Ga]Ga-**3** was tested with PCa cell lines PC-3 and LNCaP for its affinity for GRPR and PSMA receptors, lipophilicity, for its cell-binding specificity, time kinetic binding affinities and cell-internalization. Heterodimer **3** showed specific cell binding, similar affinities for PSMA receptor and GRPR and higher lipophilicity compared to monomers PSMA-617 (**1**) and RM2 (**2**), while total internalization rates and cell-binding were superior over monomers. Docking calculations showed that the PSMA-617 (**1**) /RM2 (**2**) heterodimer **3** can have binding interactions of PSMA-617 (**1**) inside the PSMA receptor funnel and of RM2 (**2**) inside the GRPR. *In vivo* biodistribution studies for [^{68}Ga]Ga-**3** showed dual targeting of PSMA-positive tumors and GRPR-positive tumors and fast pharmacokinetic properties, higher cancer cell-uptake and lower kidney uptake in comparison to the monomers.

Keywords: Prostate cancer, molecular dynamics simulations, homology modelling, induced-fit docking, PSMA, GRPR, PC-3, LNCaP, ^{68}Ga, cell-binding specificity, cell-internalization, radiolabelling, PET imaging

Introduction

Prostate cancer (PCa) is the most common malignancy worldwide in men, with persistently high numbers of patients dying from the disease. [1–3] The over-expression of certain antigens on the surface of PCa cells has been vastly utilized in Nuclear Medicine (NM) for antigen-targeted imaging and/or therapy.[4,5] The prostate specific membrane antigen (PSMA) [6–9] and gastrin releasing peptide receptor (GRPR) [10–16] are two examples, which have been utilized for the design of numerous diagnostic and therapeutic ligands, as well as for theranostic applications in NM with ligands, which can be labelled either with diagnostic nuclides for single-photon emission computerized tomography (SPECT) or positron emission tomography (PET) imaging or with therapeutic nuclides emitting beta or alpha particles (resulting in single or double strain DNA damage)[17]

PSMA or glutamate carboxypeptidase II (GCPII) is a binuclear zinc metallopeptidase protein expressed in normal prostate cells as a truncated form (PSM') lacking the intracellular and transmembrane domains of PSMA[18] and in PCa cells as a membrane protein, expressed on the cell-surface, which eventually is over-expressed in high-grade and metastatic PCa.[8,19] However, a loss of PSMA expression has also been noted, sometimes related with the progression of the malignancy from the androgen-dependent to the androgen-independent stage, while there are also reports for elevated PSMA expression related with androgen deprivation treatments.[20,21]

The first PSMA crystal structures were reported more than 15 years ago,[7,22] and now more than 80 x-ray crystallographic PSMA structures have been published or deposited in the Protein Data Bank, mainly for HO-Glu-urea-Lys and analogs. [23–26] However, PSMA-11 and PSMA-617 were the molecules that tipped the scale in favor of PSMA as a target. [16,27–31] Thus, PSMA-11 was radiolabelled with ^{68}Ga (emission of β+ radiations and X-rays) to obtain [^{68}Ga]Ga-PSMA-11 (international nonproprietary name: gozetotide) for PET imaging towards the prostate cancerous lesions in men. PSMA-617 (vipivotide tetraxetan) was radiolabelled with ^{68}Ga to obtain [^{68}Ga]Ga-PSMA-617 for PET imaging or with ^{177}Lu (beta particle therapy) or ^{225}Ac (alpha particle therapy) to obtain [^{177}Lu]Lu-PSMA-617 or [^{225}Ac]Ac-PSMA-617, respectively, for therapeutic applications. [16,27–31] Both [^{68}Ga]Ga-PSMA-11 or [^{177}Lu]Lu-PSMA-617 were licensed by Novartis, approved for medical use in the European Union in December 2022, and sold under the brand Locametz and Pluvicto, as radiopharmaceutical medications used for diagnosis of prostate cancer or for the treatment of PSMA-positive metastatic castration-resistant prostate cancer (mCRPC). The latter was developed by the German Cancer Research Center DKFZ and University Hospital Heidelberg.

The membrane protein GRPR or bombesin receptor subtype 2 (BB2R), a G-coupled protein receptor (GPCR), has been considered as target for PCa, especially for locally recurrent PCa after brachytherapy and

external beam radiotherapy. [11–13,15,16,32–34] GRPR is over-expressed in PCa, in comparison to sparse expression in normal prostate tissue, while its expression increases in well-differentiated carcinomas and is correlated with the process of prostate cell transformation into malignant neoplasms. [12,15,16,33–36]

One of the most studied GRPR ligands coupled with a chelator is the GRPR specific antagonist DOTA-(4-amino-1-carboxymethyl-piperidine)-*D*-Phe^6-Gln^7-Trp^8-Ala^9-Val^{10}-Gly^{11}-His^{12}-Sta^{13}-Leu^{14}-NH_2 (**2**) or RM2 (**2**) (i.e. DOTA-4-amino-1-carboxymethylpiperidine-[*D*-Phe^6,Sta^{13},Leu^{14}]-BN(6−14); the peptide amino acids numbering correspond to the full 14-amino acid peptide agonist bombesin (BN)). Radiolabelled RM2 (**2**), i.e., [^{68}Ga]Ga-**2** (Scheme 1) has entered clinical trials for diagnosis and treatment of PCa and BCa[12,37,38]

Since prostate cancer cells usually express both PSMA and GRPR a heterodimeric molecule, combining both specificities, may improve the sensitivity of PSMA-targeted prostate cancer imaging. While 95% of all prostate cancers express PSMA, GRPR is overexpressed in 84% of all human prostate cancers.[1] GRPR expression can be found in the majority of lymph node metastases and in 52.9% of bone lesions. Compared to benign prostate tissue, GRPR expression is higher in malignant lesions. Moreover, as the expression of GRPR was reported to be enhanced in early-stage prostate cancers and lower in high grade disease, the expression profile of GRPR seems to be contrary to PSMA which is higher in later and poorly differentiated stages of the disease. Thus, the combination of these two specificities for the diagnosis and therapy of prostate cancer might be of high clinical impact. The accuracy of imaging prostate cancer and its disseminated metastases might profit from the here presented bispecific PSMA-/GRPR-targeted radiotracer.

The need to achieve a higher tumor-binding for the ligands and the need to address the problem of tumor heterogeneity gave birth to the idea of heterodimeric ligands, which can bind in two different receptors.[39–41] A low molecular weight heterodimer consists of two covalently linked peptides or peptidomimetics combining specificities for two different antigens/epitopes, e.g. PSMA/GRPR, while for the purposes of molecular imaging, a chelator group (i.e., the open chelator HBED-CC[42,43], NOTA[44,45], DOTA[46] , DO3A[47]) for radiometal complexation, is usually included in the structure.[40,45,48] Various linkers have been utilized consisting of a carbon chain (i.e., 5-Ava, 6-Ahx, 8-Aoc, or AMBA)[47] or an amino acid chain $(HE)_n$, (n = 1-3, and of H = histidine, E = glutamic acid)[43], or PEG_n (PEG = polyethylene glycol)[45], X-triazolyl-Tyr-PEG_2 (X = 0, -PEG_2-, -$(CH_2)_8$-))[49] to connect the pharmacophores with the chelator group; primarily aiming to increase the distance between the two parts of the heterodimer, and thus ensuring a minimal interference of the chelator group with the binding properties of the pharmacophore;[33,39] and secondarily to modify and improve the pharmacokinetic properties of the heterodimers[40,42,50] . Most examples of heterodimers targeting PSMA/GRPR [27,40,48] used either Lys-urea-Glu-OH or HO-Glu-urea-Glu-OH (DUPA = (2-[3-(1,3-dicarboxypropyl)-ureido]pentanedioic acid), for targeting PSMA and truncated BN analogs[42,44,45,49] for targeting GRPR, the latter with agonistic (i.e., H_2N-PEG_2-[D-Tyr^6,beta-Ala^{11},Thi^{13},Nle^{14}]BN(6-14)[42,43], Lys^3-Bombesin[46]) or antagonistic activity (i.e., RM26[44,45,49]).

In the present study, we synthesized a heterodimer (**3**) using the core structures of PSMA-617 (**1**), and RM2 (**2**) ligands (**Scheme 1**) and the DOTA chelator. Compound **1** was synthesized using Solid Phase Peptide Synthesis (SPPS) with an azide arm, while **2** with an alkyne pending arm; the two parts were connected using copper catalyzed click chemistry (CuAAC), and then the chelator was attached to give **3**. The heterodimer **3** was radiolabelled with the diagnostic radionuclide ^{68}Ga and the therapeutic ^{177}Lu, and tested *in vitro* for its affinity, time kinetic binding affinities and internalization studies in PCa cell lines PC-3 (GRPR+, PSMA-) that overexpressed GRPR and LNCaP cell lines (PSMA+, GRPR-) that overexpressed PSMA. As controls in all *in vitro* studies, we used the respective monomers i.e., PSMA-617 and RM2 or the respective ^{68}Ga-labelled ligands. The [^{68}Ga]Ga-**3** (^{68}Ga-**3**) compound was also studied for its pharmacokinetic profile and tumor targeting ability in SCID mice bearing PC-3 and LNCaP tumors.

Results

Chemical Synthesis

Synthesis of pharmacophores **1** and **2** was accomplished using SPPS on a 2-chloro-trytyl-resin and rink amide resin, respectively, as outlined in **Scheme 2**. Amino acid coupling was carried out using HBTU/DIPEA according to standard Fmoc peptide synthesis protocols we previously applied.[43,51] The PSMA-specific azido-PSMA-617 analog (**1**) and GRPR specific alkyno-RM2 analog (**2**) were each cleaved from the resin with TFA/TIPS/H_2O, purified by RP-HPLC (Supporting Information) and analyzed with MALDI-MS (**Table 1**). In the next step they reacted with a CuAAC reaction and the **1**/**2** conjugate was coupled with DOTA-mono-N-hydroxysuccinimide ester (DOTA-NHS-ester) resulting in the heterodimer **3**, which was purified with RP-HPLC and analyzed with MALDI-MS (see Methods Section).

Radiolabelling

The heterodimer **3** and the two monomers, PSMA-617 (**1**) and RM2 (**2**), were labeled with the PET diagnostic radiometal ^{68}Ga [half-life ($T_{1/2}$) = 68 min; maximum energy of positrons (b1) = 1.9 MeV [88%]) in HEPES (N-2-hydroxyethylpiperazine-N-2-ethane sulfonic acid) buffer resulting in [^{68}Ga]Ga-PSMA-617, [^{68}Ga]Ga-RM2, [^{68}Ga]Ga-**3** and were also labeled with the therapeutic ^{177}Lu ($T_{1/2}$ = 6.71 d; maximum energy of electrons

[β^-] = 497 keV [79%]; energy of photons (γ) = 113 keV [6%]; roentgen radiation (x) = 208 keV [11%]) in sodium acetate (Na-Ac) buffer resulting in [^{177}Lu]Lu-PSMA-617, [^{177}Lu]Lu-RM2, [^{177}Lu]Lu-**3**. The results of the radio RP-HPLC analysis are presented in **Figure 1**. In all cases, the PSMA-617 (**1**) was eluted first and the heterodimer **3** last, which was in accordance with the size of each ligand. Radiochemical purity in all cases was above 95%, while radiochemical yield was over 90%.

Determination of lipophilicity

The lipophilicities of all compounds, i.e. [^{68}Ga]Ga-PSMA-617, [^{68}Ga]Ga-RM2, [^{68}Ga]Ga-**3** and [^{177}Lu]Lu-PSMA-617, [^{177}Lu]Lu-RM2, [^{177}Lu]Lu-**3** were determined by measuring their equilibrium distribution in a two-phase system consisting of n-octanol and phosphate buffer solution (PBS) with pH 7.4. The results of the logD distribution coefficient were presented in **Table 2**. In all cases negative logD values were observed showing the preference of all compounds for the water phase, however in both cases the monomers were more hydrophilic than the heterodimer **3,** which also showed negative logD values but closer to zero. This agreed with previously mentioned results from the radio RP-HPLC analysis.

Determination of affinity for PSMA and GRPR

The inhibition potency (IC_{50}) of heterodimer **3** was determined by a cell-based competitive assay with LNCaP (PSMA+, GRPR-) and PC-3 cells (PSMA-, GRPR+). For LNCaP cells the heterodimer **3** and control PSMA-617 (**1**) at various concentrations (C = 0-5000 nM) were competed for PSMA receptor binding with [^{68}Ga]Ga-PSMA-10 (IC_{50} = 3.8 ± 1.8 nM, $C_{[Ga\text{-}68]Ga\text{-}PSMA\text{-}10}$ = 0.75 nM),[59] while for PC-3 cells the heterodimer **3** and control RM2 (**2**) at various concentrations (C = 0-5000 nM) were competed against GRPR with ^{125}I-bombesin (IC_{50} = 0.4 nM, $C_{[I\text{-}125]I\text{-}BBN}$ = 50 pM).[60] Each value was measured in quadruple and the competitive binding curves are presented in **Figure 2**. The IC_{50} values for **3** and controls are summarized in **Table 3**. For PSMA the affinity of PSMA-617 (**1**) was IC_{50} = 6.41 nM and of **3** was 3-fold lower (IC_{50} = 21.41 nM), while for GRPR the affinity of RM2 (**2**) was IC_{50} = 45.59 nM and of **3** was equal (IC_{50} = 43.93 nM).

Time kinetic cell binding

Time kinetic data for heterodimer [^{68}Ga]Ga-**3** (30 nM in 1.4 × 10^5 cells) and control [^{68}Ga]Ga-PSMA-617 for LNCaP (PSMA+, GRPR-) cells and control [^{68}Ga]Ga-RM2 for PC-3 (PSMA-, GRPR+) cells, were investigated in the time range of 0−120 min, while blocking studies were also conducted, and the results are presented in **Figure 3**. For each case the heterodimer **3** was investigated in parallel with the suitable monomer for each receptor/cell line. The heterodimer [^{68}Ga]Ga-**3** presented specific cell binding, in both cell lines LNCaP and PC-3, while a minimization of cell bound radioactivity was observed during the blocking experiments (**Figure 3A, C**), providing proof for the specificity of cell-binding. The heterodimer, [^{68}Ga]Ga-**3** in all cases presented higher cell-uptake in the same experimental conditions in comparison to the monomers (controls) (**Figure 3B**, **3D**).

Internalization

The fractions of surface-bound and internalized radio-ligand were determined after incubation of each ^{68}Ga-labeled tracer, i.e. [^{68}Ga]Ga-**3** and monomers [^{68}Ga]Ga- PSMA-617 and [^{68}Ga]Ga-RM2 tested as controls in the assay, with LNCaP and PC-3 cells for 45 min, at 37 ^{o}C and at 4 ^{o}C. The results of cell bound radioligand are presented in **Figure 4A** and **4C** for LNCaP cells and in **Figure 4B** and **4D** for PC-3 cells. The percentage of total bound radioligand for the heterodimer [^{68}Ga]Ga-**3** was higher in both PC-3 and LNCaP cell lines in comparison with the monomers for all time points studied. In both cases the heterodimer [^{68}Ga]Ga-**3** was able to specifically bind in both receptors PSMA (LNCaP cells) and GRPR (PC-3 cells). The majority of [^{68}Ga]Ga-**3** was surface bound. The amount of internalized and surface bound fraction of heterodimer **3** for each cell line LNCaP and PC-3 was in both cases higher or comparable with the corresponding monomers PSMA-617 (**1**) and RM2 (**2**).

Specifically, for PC3 cells (expressed as % of added radioactivity) were: (sb) 0.46 ± 0.10 %, and (int) 0.18 ± 0.30 %) at 37 ^{o}C, and (sb) 0.50 ± 0.09 % and (int) 0.08 ± 0.01 % at 4 ^{o}C. For LNCaP cells, (sb) 1.12 ± 0.02 %, and (int) 0.68 ± 0.04 % at 37 ^{o}C, and (sb) 0.95 ± 0.15 % and (int) 0.19 ± 0.04% at 4 ^{o}C. As expected, at 4 ^{o}C energy-dependent internalization was minimized, while the surface-bound fraction remained practically the same. In addition, the percentage of bound ligand **3** for the LNCaP cells was much higher than for the PC-3 cells.

Biodistribution

The pharmacokinetic profile and tumor targeting ability of the radiolabeled heterodimer [^{68}Ga]Ga-**3** was examined with organ distribution experiments (30, 60 and 120 min p.i.) in Swiss albino mice bearing PC-3 (**Figure 5A**) and LNCaP (**Figure 5B**) tumors. The heterodimer [^{68}Ga]Ga-**3** showed fast blood clearance, while it was mainly excreted *via* the kidneys into the urinary bladder. Tumor uptake was higher for the LNCaP tumors than for PC-3 tumors, which can be attributed to the higher expression of PSMA in LNCaP cells in comparison to the one of GRPR in PC-3 cells. In addition, the amount of [^{68}Ga]Ga-**3** inside the LNCaP tumors did not degrade as fast as the respective one in the PC-3 tumors, possibly because of the higher rates of internalization for the PSMA ligand-receptor complexes than for the GRPR antagonist complexes. Considering the increased expression of PSMA in the kidneys, the kidney uptake was much lesser than in other heterodimers we previously developed that ranged between 66-122% IA/g. [51,52] The observed off-targeting uptake in the pancreas was due to the normal expression of GRPRs in this tissue and was gradually degraded with time in a faster rate than the activity located in the tumors. In general, [^{68}Ga]Ga-**3** showed dual targeting of PSMA-positive tumors and GRPR-positive tumors and fast clearance from the body, while in comparison to the monomers[2,3] a higher cancer cell-uptake and lower kidneys uptake was observed.

Docking calculations

The docking poses of the PSMA-617 part or the RM2 part of the heterodimer (**3**) into the binding area of PSMA receptor or BBR2 were performed as previously described in ref. Liolios et al.[52] and are shown in **Figure 6.**

Discussion

The majority of human tumors display heterogeneity in their morphological and/or physiological features i.e., expression of cell surface receptors, proliferative and angiogenic potential.[53] Specifically, for nonendocrine tumors i.e., breast, prostate, and brain tumors, which concomitantly express several G protein–coupled receptors at a high density the application of low molecular weight heterobivalent or heteromultivalent ligands, has been propose in order to address problems of cancer targeting for diagnosis and therapy.[39] In this regard, several examples of heterodimers showing synergistic tumor targeting have been reported.[40,41,48]

One of the cases that PCa tumors show heterogeneity refers to the inharmonious expression of PSMA and GRPR, which also reflects their biodiversity. Lack of detecting either receptor expression may significantly

reduce image quality and detection ability of the PCa-associated lesion.[53–55] Since PCa cells express both receptors, a new approach, which will enhance the sensitivity of PET imaging of biochemically recurrent PCa and increase the clinical significance of the diagnostic examination can be the development of heterodimeric molecules combining both specificities.[27,40,56]

Two cases of heterodimers existed with Lys-CO-Glu-OH pharmacophore for PSMA receptor and the GRPR agonist H_2N-PEG_2-[*D*-Tyr^6,*beta*-Ala^{11},Thi^{13},Nle^{14})BN(6-14) (Nle = norleucine, Thi = 3-thienylalanine) covalently connected with the HBED-CC chelator linked *via* its two carboxylic groups (not participating at the metal complexation) with either one of the pharmacophores.[42,43] The BN peptidic analogue used in those cases was structurally relevant to the resistant to the peptidases BN analogue used in the clinically tested [^{68}Ga]GaBZH$_3$ (BZH$_3$ = DOTA-PEG_2-[D-Tyr^6, *beta*-Ala^{11}, Thi^{13}, Nle^{14}] BN(6-14) amide).[57,58] These heterodimers showed high affinity values for both PSMA and GRPR targets, with higher uptake for both kinds of PCa cells studied (e.g., PC-3, 4.40 - 9.00 nM, and LNCaP, 17.4 – 42.4 nM) and specific tumor uptake in LNCaP and AR42J xenographs thus,[42,43] having a clear advantage regarding previous studied monomers. However, while the 1st generation of heterodimers (HE_{00})[42] showed high kidney uptake (164.38 % IA/g, 1h p.i.). The addition of the $(HE)_n$ (n = 1-3) amino acid spacer between the HBED-CC chelator and the PSMA pharmacophore (HE_{0-3}) not only reduced the kidney (73.25-87.57% IA/g, 1hr p.i.) uptake but in some cases improved the tumor uptake resulting in higher values than the respective monomers.[43]

Another ^{68}Ga-labelled heterodimeric radiotracer, [^{68}Ga]Ga-iPSMA-BN consisted from the iPSMA (Lys(Nal)-urea-Glu-OH; Nal = 3-(1-naphthyl)-L-alanine) oligopeptide and the Lys^3-BN(1-14) peptide agonist, both linked to a DOTA chelator.[46] Heterodimer [^{68}Ga]Ga-iPSMA-BN showed superiority against each monomer, [^{68}Ga]Ga-iPSMA and [^{68}Ga]Ga-BN, in both cell lines and animal models. .[46] The ligand was also labelled with ^{177}Lu and evaluated *in vitro* (LNCaP and PC-3 cells), with *ex vivo* biodistributions and Micro-SPECT/CT imaging studies in xenographed mice, which proved the positive influence of the heterobivalent effect.[59] Additionally, biokinetics and dosimetry data has been obtained for [^{68}Ga]Ga-iPSMA-BN in a study of 4 healthy volunteers showing specific uptake in the pancreas (GRPR expressing) and salivary glands (PSMA expressing).[60]

Three additional bispecific heterodimers based on the antagonistic peptide RM26 (*D*-Phe^6-Gln^7-Trp^8-Ala^9-Val^{10}-Gly^{11}-His^{12}-Sta^{13}-Leu^{14}-NH_2) for GRPR and PSMA-617 (**1**) were developed, [49] using the general structure: PSMA-617-X-triazolyl-Tyr-PEG_2-RM26 (X = 0, PEG_2, $(CH_2)_8$), where the two pharmacophores were linked *via* the spacer X-triazolyl-Tyr-PEG_2. The resulting heterodimers were radio-iodinated [^{125}I]I and evaluated *in vitro* and i*n vivo* in PC-3 (IC_{50} = 6.0 - 20.0 nM) and LNCaP and PC-3 PIP (IC_{50} = 80.0 - 100.0 nM) (PSMA/GRPR positive) xenographs. All resulting heterodimers showed binding specificity, cellular retention, and affinity, while among them the [^{125}I]I-PSMA-617-PEG_2-triazolyl-Tyr-PEG_2-RM26 presented the highest values regarding cancer cell uptake. Further evaluated in vivo in PCa xenographs was also in its favor referring to higher tumor accumulation

(PC-3, 4.3 %ID/g, PC-3 PiP 10 %ID/g at 1 h p.i.), however, it showed high kidney radioactivity values (66 %ID/g and 56 %ID/g, respectively).[49]

In the present study, heterodimer **3** consisted of a PSMA-specific pharmacophore (**4**) with a linker similar to the one used in PSMA-617 (**1**), which was coupled to a GRPR specific pharmacophore similar to the RM26 pharmacophore and linker. The universal DOTA chelator which was utilized replaced the HBED-CC chelator, which was used in previous heterodimers developed from our group (HE_{00}-HE_3)[42,43] in order to provide a theranostic potential to the ligand since [^{68}GaGa-HBED-CC] can only be utilized for diagnosis (Scheme 1). Heterodimer **3** was quantitatively labeled with ^{68}Ga and ^{177}Lu, presenting optimal radiochemical purity and yield (< 95% and <90%), which is a crucial requirement for a possible future application as a theranostic agent. Heterodimer **3** showed slightly higher lipophilicity in comparison to the monomers possibly due to the increase in MW. After *in vitro* testing in LNCaP and PC-3 cells, heterodimer **3** showed similar affinities for PSMA receptor and GRPR to both control monomers PSMA-617 (**1**) and RM2 (**2**), respectively (**Figure 2**, **Table 2**). The affinity of **3** in comparison with other ligands is also summarized in **Table 2**. Differences in the IC_{50} or Ki values for the same ligands (i.e. PSMA-617, RM2) are expected due to the different platforms and protocols of experimentation. Further *in vitro* assays established the specificity of ligand [^{68}Ga]Ga-**3** for both PSMA and GRPR, while total internalization rates and its cell-binding showed superiority over both monomers (**Figures 3**-**4**).

In vivo biodistribution studies of [^{68}Ga]Ga-**3** presented generally high tumor accumulation in comparison to off-target organ radio-activity (**Figure 5**), while excretion of the ligand was mainly through the kidneys. Tumor accumulation for both tumor-models LNCaP and PC-3 peaked at 30 min, afterwards slowly degraded (60 min) and then remained at the same levels (120 min). The significantly higher levels of accumulation in LNCaP tumors in comparison with PC-3 can be attributed to the significantly higher levels of expression of PSMA/cell than of GRPR/cell.[92] Off-target radioactivity due to [^{68}Ga]Ga-**3** was also observed for the pancreas due to the overexpression of GRPR protein in this tissue. Such off-target accumulation has also been described for previously studied heterodimers, e.g. [^{68}Ga]Ga-iPSMA-BN, in human healthy volunteers.[72]

Conclusion

In the present study, a PSMA-specific scaffold, based on of PSMA-617, was combined with the GRPR specific scaffold of RM26 pharmacophore, and the DOTA chelator, to give heterodimer **3**. The radiolabeling of Heterodimer **3** was simple and with high yields for both ^{68}Ga/^{177}Lu, rendering it suitable for theranostic applications. Ligand **3** showed similar affinities for PSMA receptor and GRPR in comparison with both control monomers PSMA-617 and RM2, respectively, while in comparison with previously studied heterodimeric ligands the results of **3** were comparable. Additional *in vitro* assays established further the specificity of [^{68}Ga]Ga-**3** for

PSMA/GRPR, while total internalization rates and its cell-binding showed superiority over both monomers. The *in vivo* high tumor accumulation of [^{68}Ga]Ga-**3** in comparison to low off-target organ radio-activity makes **3** a suitable candidate for further studies for its utilization as PET-imaging agent in human subjects. These results will also trigger further studies on the utility of [^{177}Lu]Lu-**3** complex for therapeutic purposes.

Materials and Methods

Chemistry

General

All commercially available chemicals were of analytical grade and were used without further purification. The chemical suppliers were: Sigma-Aldrich (Taufkirchen, Germany) and Merck (Darmstadt, Germany), unless otherwise indicated. Protected amino acids (a.a.) and resins were supplied from Novabiochem (Merck, Darmstadt, Germany) and IRIS Biotech. (Marktredwitz, Germany). For all reaction products the chemical purity was greater than 95% as determined by RP-HPLC.

The following RP-HPLC systems were used: (a) for purifications, VWR International, La Prep UV/vis detector P314, pumps P110, column: Nucleodur Sphinx RP, 5 µm VP 250/21 (MACHEREY-NAGEL GmbH & Co. KG, Düren, Germany), gradient used (A-B): 10−90% B in 20 min, flow: 20 mL/min, (A) 0.1% TFA in H_2O and (B) 0.1% TFA in AcCN. (b) for analysis: Agilent 1100 series, multiwavelength detector (MWD), *γ*-detector (Bioscan; Washington, USA), analytical column: Chromolith RP-18e (4.6 mm × 100 mm; Merck, Darmstadt, Germany), gradient used (A−B) 0−100% B in 6 min, flow: 4 mL/min. Mass spectrometry was performed with a MALDI-MS Daltonics Microflex system (Bruker Daltonics, Bremen, Germany). Full-scan single mass spectra were obtained by scanning m/z = 200−4000 (2,5- dihydroxybenzoic acid in H_2O/AcCN 1:1 was used as matrix). For all *in vitro* and *in vivo* experiments, a NaI (TI) γ counter (Packard Cobra II, GMI, Minnesota, USA) was used for the measurement of radioactive probes.

Compound preparation

Molecules **4** and **5** were synthesized on a 2-chloro-trityl resin (C = 1.22 mmol/g, 100-200 mesh), Rink amide resin (200−400 mesh) (Merck, Darmstadt). Amino acid coupling was according to standard Fmoc peptide synthesis protocols (amino acid/HBTU/DIPEA, 4.0/3.9/4.0 equiv, 30 min, rt), while Fmoc was removed by washing resin with dimethylformamide (DMF)/piperidine (1:1, v/v, 3x 1.0 mL/ 5 min). At the final step the peptides were cleaved from the resin with the following mixture TFA/TIPS/H_2O (95/2.5/2.5, v/v/v), precipitated in ice-cold (0 °C) diethyl ether, and purified with semipreparative HPLC (see also SI for the RP-HPLC analysis of **4** and **5**). The coupling of the chelator DOTA-NHS (1.5 equiv.) (2,2',2"-(10-(2-((2,5-dioxopyrrolidin-1-yl)oxy)-2-oxoethyl)-1,4,7,10-tetraazacyclododecane-1,4,7-triyl)triacetic acid, CheMatech, Dijon, France) was accomplished with EDC (1.5 equiv) (1-ethyl-3-(3-dimethylaminopropyl)carbodiimide hydrochloride) in PBS (pH= 8.5) (**Scheme 1**). Compounds 4,5 and 3 were purified by RP-HPLC and analyzed with MALDI-MS (**Table 4**).

Radiolabeling

The heterodimer DOTA-RM2-617 and the two monomers, PSMA-617 and DOTA-RM2, were labeled with the PET diagnostic radiometal ^{68}Ga and the therapeutic ^{177}Lu.

^{68}Ga labeling: Briefly (0.3−1.0 nmol) of each precursor in 0.1 M HEPES buffer, (pH = 7.5, 100 µL), were incubated with a mixture of HEPES buffer (2.1 M, 10 µL) and 40 µL (80−100 MBq) ^{68}Ga (eluted from a ^{68}Ge/^{68}Ga generator based on pyrogallol resin support as [^{68}Ga]$GaCl_4$). The pH of the labeling solution was adjusted to pH = 4.2 using 30% NaOH and the reaction mixture was incubated at 98 °C for 15 min.

^{177}Lu labeling: ^{177}Lu was obtained from PerkinElmer as [^{177}Lu]$LuCl_3$ in 0.05 M HCl. To the [^{177}Lu]$LuCl_3$ (5 µL, 20 MBq) an amount of Na-Ac (115 µL, 400nM, pH: 5.0) was added and of 0.1–1 mM of each substance (~5 nmol) the reaction mixture was left to incubate at 98 °C for 25 min. Labeling efficiency in all cases was determined via analytical RP-HPLC.

Determination of lipophilicity

An aliquot of each ^{68}Ga-ligand (20 µL) i.e., [^{68}Ga]GaPSMA-617, [^{68}Ga]GaRM2, [^{68}Ga]Ga-**3** and [^{177}Lu]LuPSMA-617, [^{177}Lu]LuRM2, [^{177}Lu]Lu-**3** was added to a mixture of PBS (pH = 7.4, PAN-Biotech, Aidenbach, Germany) /1-octanol (Allchem GmbH Chemikalienvertrieb, Breisach, Germany) (1:1, v/v, 500 µL and 500 µL), rigorously vortexed and centrifuged (2800 rpm/8 min) and the radioactivity of each phase (aliquot of 40 µl) was measured with a gamma-counter Cobra II (PerkinElmer, Waltham, Massachusetts). The lipophilicities of all

compounds were determined by their equilibrium distribution in the two phases according to the distribution coefficient log D:

$$logD_{n-octanol/PBS} = log\frac{[solute]^{ionized}_{octanol} + [solute]^{nonionized}_{octanol}}{[solute]^{ionized}_{PBS} + [solute]^{nonionized}_{PBS}}$$

where:

$[solute]^{ionized}_{octanol}$ is the concentration of ionized compound in the n-octanol phase and $[solute]^{nonionized}_{octanol}$ of the nonionized ligand in n-octanol phase, and $[solute]^{ionized}_{PBS}$ is the concentration of ionized compound in PBS, and $[solute]^{nonionized}_{PBS}$ is the concentration of nonionized ligand in PBS. Each measurement was performed in triplicates and results were expressed as Means ± Standard deviation.

Biological testing

Cell Culture & cell assays

In vitro and *in vivo* experiments were performed with the following cell lines: the GRPR positive PC-3 cells (bone metastasis of a grade IV prostatic adenocarcinoma, ATCC CRL- 1435) and the PSMA-positive LNCaP cells (ATCC CRL-1740), which were cultured in DMEM and RPMI 1640 medium, respectively supplemented with 10% fetal calf serum and 2 mM L-glutamine (Invitrogen, Carlsbad, CA, USA). Cells were grown at 37 °C in humidified air with 5% CO_2. Trypsin-ethylenediaminetetraacetic acid (trypsin- EDTA; 0.25% trypsin, 0.02% EDTA, Invitrogen) was used for cell harvesting.

Determination of Binding Affinity for PSMA in LNCaP and PC-3 cells

The assays were performed according to previously described methods.[93,94] Briefly, LNCaP 10^5 cells per well were incubated with a solution of ^{68}Ga-labeled radioligand [Glu-urea-Lys(Ahx)]$_2$-HBED-CC (0.75 nM, PSMA-10, precursor purchased from ABX, Radeberg, Germany) and an ascending series of 12 different analyte concentrations (0, 0.5, 1, 2.5, 5, 10, 25, 50, 100, 500, 1000 and 5000 nM, 100 µL/well in Optimem, 45 min). This mixture was removed after incubation and the wells were washed on a multiscreen vacuum manifold (Millipore, Billerica, MA) three times with PBS. The following detection of cell-bound radioactivity was measured using a gamma counter (Packard Cobra II, GMI, Minnesota, USA). Data was fitted with a nonlinear regression algorithm (GraphPad Software) to determine the 50% inhibitory concentration (IC_{50}) values.

A similar procedure was followed for PC-3 cells.[60,93] A population of 10^5 PC-3 cells /well was incubated with ^{125}I-[Tyr^4]-BN ([^{125}I]I-BBN C = 50 pM, 722kBq (19,4µCi), 72,2GBq/µmol, Perkin Elmer) and an ascending series

of 8 different analyte (**3**) concentrations (0, 0.025, 0.25, 2.5, 25, 125, 250, 1250, 12500 nM) for 45 min. After incubation the mixture was removed, the wells were washed with PBS and the cell-bound radioactivity was measured using a gamma counter (Hidex AMG - Automated Gamma Counter). Data was fitted with a nonlinear regression algorithm (GraphPad Software) to determine the 50% inhibitory concentration (IC_{50}) values.

Time Kinetic Cell Binding

Specificity of binding in relation with time was analyzed using a modified protocol[95]. Solutions of the ^{68}Ga-labeled compounds (30 nM, 30 MBq/nmol), were added to 1 × 10^6 cells (PC-3) suspended in 0.1 mL Opti-MEM (Gibco, Auckland, New Zealand) and incubated at 37 °C. Samples were briefly vortexed and a 10 µL aliquot (1-1.4 × 10^5 cells) was taken at predetermined time points: 15, 30, 45, 60, 90 min. The aliquot was then transferred to a 400 µL microcentrifuge tube (Roth, Germany) containing 350 µL of a 75:25 mixture of silicon oil, density 1.05 (Sigma Aldrich, Germany), and mineral oil, density 0.872 (Acros, Nidderau, Germany). Separation of cells from the medium was performed by centrifugation at 12000 rpm for 2 min. After freezing the tubes using liquid nitrogen, the bottom tips containing the cell pellet were cut off. The cell pellets and the supernatants were separately counted in a γ counter. Non-specific binding was determined by adding a 1000-fold excess of a blocking substance BN or H_2N-PEG_2-4-amino-1-carboxymethylpiperidine-[(R)-Phe^6,Sta^{13},Leu^{14}]-BN(6–14), 100 mM solution in DMSO. Cell binding (cell counts) was determined as the percentage of the total counts added to the cell suspension (counts for tip and top).

Internalization Experiments in PC-3 and LNCaP Cells

Internalization experiments were performed as previously described.[93,94] Briefly, 10^6 PC-3 or LNCaP cells were seeded in 6-well cell culture plates 24 h before the day of the experiment. The cells were incubated with the radiolabeled compounds (30 nM, in reduced serum, Opti-MEM, Gibco) for 45 min at 37 and 4 °C, respectively. To determine specific cellular uptake, cells were blocked by competition with 1000-fold excess of GRPR block: H_2N-PEG_2-4-amino-1-carboxymethylpiperidine-[D-Phe^6,Sta^{13},Leu^{14}]-BN(6−14) (C = 30 µM/Well) and PSMA block: 2-PMPA (2-(phosphonomethyl)pentane-1,5-dioic acid) (C = 500 µM/well). After incubation the supernatant was removed and the cells were washed with ice-cold PBS. To remove surface-bound radioactivity, cells were incubated twice with 0.5 mL of glycine-HCl in PBS (50 mM, pH 2.8) for 5 min. Then cells were washed with 1.0 mL of ice-cold PBS and lysed using 0.5 mL of 0.3 N NaOH (internalized radioactivity). The surface-bound and the internalized fraction were measured in a *γ* counter (Packard Cobra II, GMI, Ramsey, MN, USA).

Biodistribution

Tumor xenographs were created by subcutaneously inoculation of 5×10^6 cells of PC-3 or LNCaP (in 50% Matrigel; Becton Dickinson, Heidelberg, Germany) into the right trunk of 7- to 8-week-old SCID mice to obtain the experimental xenograft tumor models. Tumors were allowed to grow to approximately 300 mm^3 in size. Each of the ^{68}Ga-labeled compounds was injected into a tail vein (1−2 MBq; 60 pmol). Syringes were measured before and after administration and appropriate corrections were made for the calculation of the injected dose (ID). The animals were euthanized by isofluorane inhalation at predetermined time points (30 min, 60 min and 90 min) post injection. The dissected major organs along with blood and muscle samples were excised and measured. The radioactivity uptake was measured with a gamma counter and calculated as % ID/g. The % IA in whole blood was estimated assuming a whole blood volume of 6.5% of the total body weight. All animal experiments complied with the current laws of the EU.

Abbreviations

GCPII, glutamate carboxypeptidase II; GRPR, gastrin releasing peptide receptor; GUI, graphical user interface; MD, molecular dynamics; NM, Nuclear Medicine; PET, positron electron tomography; PCa, prostate cancer, GRPR: gastrin releasing peptide receptor; PSMA, prostate specific membrane antigen; POPC, 1-palmitoyl-2-oleoyl-*sn*-glycero-3-phosphatidylcholine; SPECT, single-photon emission computerized tomography;

Author Information

Author Contributions

C.L. conceived the project and design experiments, MS writing. C.L., P.B. guided the research. C.L. synthesized with D.B. and M.B. compounds **1-5** in P.B. lab, performed the radiolabelling and cell assays. M.Sch performed radiochemistry experiments. B-W.Ul. performed radiolabelling and cell assays. G.L. with A.K. performed docking calculations. C.L., A.K. wrote the manuscript and K.K. edited it.

Corresponding authors

Christos Liolios, liolios.xr@gmail.com

Penepole Bouziotis, bouzioti@rrp.demokritos.gr

References

(1) Center, M. M.; Jemal, A.; Lortet-Tieulent, J.; Ward, E.; Ferlay, J.; Brawley, O.; Bray, F. International Variation in Prostate Cancer Incidence and Mortality Rates. *Eur. Urol.* **2012**, *61* (6), 1079–1092. https://doi.org/10.1016/j.eururo.2012.02.054.

(2) Jemal, A.; Siegel, R.; Xu, J.; Ward, E. Cancer Statistics, 2010. *CA. Cancer J. Clin.* **2010**, *60* (5), 277–300. https://doi.org/10.3322/caac.20073.

(3) Siegel, R. L.; Miller, K. D.; Jemal, A. Cancer Statistics, 2020. *CA. Cancer J. Clin.* **2020**, *70* (1), 7–30. https://doi.org/10.3322/caac.21590.

(4) Thundimadathil, J. Cancer Treatment Using Peptides: Current Therapies and Future Prospects. *J. Amino Acids* **2012**, *2012*, 1–13. https://doi.org/10.1155/2012/967347.

(5) Ferro-Flores, G.; Ramírez, F. D. M.; Meléndez-Alafort, L.; Santos-Cuevas, C. L. Peptides for in Vivo Target-Specific Cancer Imaging. *Mini Rev. Med. Chem.* **2010**, *10* (1), 87–97.

(6) Wolf, P. Prostate Specific Membrane Antigen as Biomarker and Therapeutic Target for Prostate Cancer. In *Prostate Cancer - Diagnostic and Therapeutic Advances*; InTech, 2011; pp 81–100. https://doi.org/10.5772/26951.

(7) Davis, M. I.; Bennett, M. J.; Thomas, L. M.; Bjorkman, P. J. Crystal Structure of Prostate-Specific Membrane Antigen , a Tumor Marker and Peptidase. *Proc. Natl. Acad. Sci. U. S. A.* **2005**, *102* (17), 5981–5986. https://doi.org/pnas.

(8) Bacich, D. J.; Pinto, J. T.; Tong, W. P.; Heston, W. D. W. Cloning, Expression, Genomic Localization, and Enzymatic Activities of the Mouse Homolog of Prostate-Specific Membrane Antigen/NAALADase/Folate Hydrolase. *Mamm. Genome* **2001**, *12* (2), 117–123. https://doi.org/10.1007/s003350010240.

(9) Israeli, R. S.; Powell, C. T.; Corr, J. G.; Fair, W. R.; Heston, W. D. Expression of the Prostate-Specific Membrane Antigen. *Cancer Res.* **1994**, *54* (7), 1807–1811.

(10) Patel, O.; Shulkes, A.; Baldwin, G. S. Gastrin-Releasing Peptide and Cancer. *Biochim. Biophys. Acta* **2006**, *1766*, 23–41. https://doi.org/10.1016/j.bbcan.2006.01.003.

(11) Cornelio, D. B.; Roesler, R.; Schwartsmann, G. Gastrin-Releasing Peptide Receptor as a Molecular Target in Experimental Anticancer Therapy. *Ann. Oncol.* **2007**, *18* (9), 1457–1466. https://doi.org/10.1093/annonc/mdm058.

(12) Dumont, R. a; Tamma, M.; Braun, F.; Borkowski, S.; Reubi, J. C.; Maecke, H.; Weber, W. a; Mansi, R. Targeted Radiotherapy of Prostate Cancer with a Gastrin-Releasing Peptide Receptor Antagonist Is Effective as Monotherapy and in Combination with Rapamycin. *J. Nucl. Med.* **2013**, *54* (5), 762–769. https://doi.org/10.2967/jnumed.112.112169.

(13) Biddlecombe, G. B.; Rogers, B. E.; de Visser, M.; Parry, J. J.; de Jong, M.; Erion, J. L.; Lewis, J. S. Molecular Imaging of Gastrin-Releasing Peptide Receptor-Positive Tumors in Mice Using 64Cu- and 86Y-DOTA-(Pro1,Tyr4)-Bombesin(1-14). *Bioconjug. Chem.* **2007**, *18* (3), 724–730. https://doi.org/10.1021/bc060281l.

(14) Veerendra, B.; Sieckman, G.; Hoffman, T.; Rold, T.; Retzloff, L.; McCrate, J.; Prasanphanich, A.; Smith, C.

Synthesis, Radiolabeling and In Vitro GRP Receptor Targeting Studies of 99m Tc-Triaza-X-BBN[7-14]NH 2 (X=Serylserylserine, Glycylglycylglycine, Glycylserylglycine, or Beta Alanine). *Synth. React. Inorganic, Met. Nano-Metal Chem. (formerly Synth. React. Inorg. Met. Chem.* **2006**, *36* (6), 481–491. https://doi.org/10.1080/15533170600778075.

(15) Sancho, V.; Di Florio, A.; Moody, T. W.; Jensen, R. T.; W. Moody, T.; T. Jensen, R. Bombesin Receptor-Mediated Imaging and Cytotoxicity: Review and Current Status. *Curr. Drug Deliv.* **2011**, *8* (1), 79–134. https://doi.org/10.2174/156720111793663624.

(16) Iagaru, A. Will GRPR Compete with PSMA as a Target in Prostate Cancer? *J. Nucl. Med.* **2017**, *58* (12), 1883–1884. https://doi.org/10.2967/jnumed.117.198192.

(17) Dadachova, E. Cancer Therapy with Alpha-Emitters Labeled Peptides. *Semin. Nucl. Med.* **2010**, *40* (3), 204–208. https://doi.org/10.1053/j.semnuclmed.2010.01.002.

(18) Yao, V.; Parwani, A.; Maier, C.; Heston, W. D.; Bacich, D. J. Moderate Expression of Prostate-Specific Membrane Antigen, a Tissue Differentiation Antigen and Folate Hydrolase, Facilitates Prostate Carcinogenesis. *Cancer Res.* **2008**, *68* (21), 9070–9077. https://doi.org/10.1158/0008-5472.CAN-08-2328.

(19) Bařinka, C.; Rojas, C.; Slusher, B.; Pomper, M. Glutamate Carboxypeptidase II in Diagnosis and Treatment of Neurologic Disorders and Prostate Cancer. *Curr. Med. Chem.* **2012**, *19* (6), 856–870.

(20) Evans, M. J.; Smith-Jones, P. M.; Wongvipat, J.; Navarro, V.; Kim, S.; Bander, N. H.; Larson, S. M.; Sawyers, C. L. Noninvasive Measurement of Androgen Receptor Signaling with a Positron-Emitting Radiopharmaceutical That Targets Prostate-Specific Membrane Antigen. *Proc. Natl. Acad. Sci.* **2011**, *108* (23), 9578–9582. https://doi.org/10.1073/pnas.1106383108.

(21) Kranzbühler, B.; Salemi, S.; Umbricht, C. A.; Müller, C.; Burger, I. A.; Sulser, T.; Eberli, D. Pharmacological Upregulation of Prostate-Specific Membrane Antigen (PSMA) Expression in Prostate Cancer Cells. *Prostate* **2018**, *78* (10), 758–765. https://doi.org/10.1002/pros.23522.

(22) Mesters, J. R.; Barinka, C.; Li, W.; Tsukamoto, T.; Majer, P.; Slusher, B. S.; Konvalinka, J.; Hilgenfeld, R. Structure of Glutamate Carboxypeptidase II, a Drug Target in Neuronal Damage and Prostate Cancer. *EMBO J.* **2006**, *25* (6), 1375–1384. https://doi.org/10.1038/sj.emboj.7600969.

(23) Navrátil, M.; Ptáček, J.; Šácha, P.; Starková, J.; Lubkowski, J.; Bařinka, C.; Konvalinka, J. Structural and Biochemical Characterization of the Folyl-Poly-γ-l-Glutamate Hydrolyzing Activity of Human Glutamate Carboxypeptidase II. *FEBS J.* **2014**, *281* (14), 3228–3242. https://doi.org/10.1111/febs.12857.

(24) Zhang, A. X.; Murelli, R. P.; Barinka, C.; Michel, J.; Cocleaza, A.; Jorgensen, W. L.; Lubkowski, J.; Spiegel, D. A. A Remote Arene-Binding Site on Prostate Specific Membrane Antigen Revealed by Antibody-Recruiting Small Molecules. *J. Am. Chem. Soc.* **2010**. https://doi.org/10.1021/ja104591m.

(25) Barinka, C.; Byun, Y.; Dusich, C. L.; Banerjee, S. R.; Chen, Y.; Castanares, M.; Kozikowski, A. P.; Mease, R. C.; Pomper, M. G.; Lubkowski, J. Interactions between Human Glutamate Carboxypeptidase II and Urea-Based Inhibitors: Structural Characterization. *J. Med. Chem.* **2008**, *51* (24), 7737–7743. https://doi.org/10.1021/jm800765e.

(26) Pavlicek, J.; Ptacek, J.; Barinka, C. Glutamate Carboxypeptidase II: An Overview of Structural Studies and Their Importance for Structure-Based Drug Design and Deciphering the Reaction Mechanism of the Enzyme. *Curr. Med. Chem.* **2012**, *19* (9), 1300–1309. https://doi.org/10.2174/092986712799462667.

(27) Neels, O. C.; Kopka, K.; Liolios, C.; Afshar-Oromieh, A. Radiolabeled PSMA Inhibitors. *Cancers (Basel).* **2021**, *13* (24), 6255. https://doi.org/10.3390/cancers13246255.

(28) Benešová, M.; Schäfer, M.; Bauder-Wüst, U.; Afshar-Oromieh, A.; Kratochwil, C.; Mier, W.; Haberkorn, U.; Kopka, K.; Eder, M. Preclinical Evaluation of a Tailor-Made DOTA-Conjugated PSMA Inhibitor with Optimized Linker Moiety for Imaging and Endoradiotherapy of Prostate Cancer. *J Nucl Med* **2015**, *56* (6), 914–920. https://doi.org/10.2967/jnumed.114.147413.

(29) Afshar-Oromieh, A.; Hetzheim, H.; Kratochwil, C.; Benesova, M.; Eder, M.; Neels, O. C.; Eisenhut, M.; Kübler, W.; Holland-Letz, T.; Giesel, F. L.; Mier, W.; Kopka, K.; Haberkorn, U. The Novel Theranostic PSMA-Ligand PSMA-617 in the Diagnosis of Prostate Cancer by PET/CT: Biodistribution in Humans, Radiation Dosimetry and First Evaluation of Tumor Lesions. *J. Nucl. Med.* **2015**, jnumed.115.161299-. https://doi.org/10.2967/jnumed.115.161299.

(30) Kopka, K.; Benešová, M.; Bařinka, C.; Haberkorn, U.; Babich, J. Glu-Ureido–Based Inhibitors of Prostate-Specific Membrane Antigen: Lessons Learned During the Development of a Novel Class of Low-Molecular-Weight Theranostic Radiotracers. *J. Nucl. Med.* **2017**, *58* (Supplement 2), 17S-26S. https://doi.org/10.2967/jnumed.116.186775.

(31) Ristau, B. T.; O'Keefe, D. S.; Bacich, D. J. The Prostate-Specific Membrane Antigen: Lessons and Current Clinical Implications from 20 Years of Research. *Urol. Oncol.* **2014**, *32* (3), 272–279. https://doi.org/10.1016/j.urolonc.2013.09.003.

(32) Smith, J. C.; Sieckman, G. L.; Owen, N. K.; Hayes, D. L.; Mazuru, D. G.; Volkert, W. A.; Hoffman, T. J. Radiochemical Investigations of [188Re(H2O)(CO)3-Diaminopropionic Acid-SSS-Bombesin(7-14)NH2]: Syntheses, Radiolabeling and in Vitro/in Vivo GRP Receptor Targeting Studies. *Anticancer Res.* **2003**, *23* (1A), 63–70.

(33) Reubi, J. C.; Maecke, H. R. Peptide-Based Probes for Cancer Imaging. *J. Nucl. Med.* **2008**, *49* (11), 1735–1738. https://doi.org/10.2967/jnumed.108.053041.

(34) Maecke, H.; Hofmann, M. 68Ga-Labeled Peptides in Tumor Imaging. *J. Nucl. Med.* **2005**, *46* (1), 172–178.

(35) Nagasaki, S.; Nakamura, Y.; Maekawa, T.; Akahira, J.; Miki, Y.; Suzuki, T.; Ishidoya, S.; Arai, Y.; Sasano, H. Immunohistochemical Analysis of Gastrin-Releasing Peptide Receptor (GRPR) and Possible Regulation by Estrogen Receptor Bcx in Human Prostate Carcinoma. *Neoplasma* **2012**, *59* (2), 224–232. https://doi.org/10.4149/neo_2012_029.

(36) Liolios, C.; Patsis, C.; Bauder-Wuest, U.; Scholl, C.; Eder, M.; Kopka, K. Relations between PSMA and GRP Receptor Expression in Prostate and Breast Cancer Cell Lines for Tumor Imaging. *J. Nucl. Med.* **2017**, *58* (supplement 1), 929–929.

(37) Mansi, R.; Wang, X.; Forrer, F.; Waser, B.; Cescato, R.; Graham, K.; Borkowski, S.; Reubi, J. C.; Maecke, H. R. Development of a Potent DOTA-Conjugated Bombesin Antagonist for Targeting GRPr-Positive Tumours. *Eur. J. Nucl. Med. Mol. Imaging* **2011**, *38* (1), 97–107. https://doi.org/10.1007/s00259-010-1596-9.

(38) Stoykow, C.; Erbes, T.; Maecke, H. R.; Bulla, S.; Bartholomä, M.; Mayer, S.; Drendel, V.; Bronsert, P.; Werner, M.; Gitsch, G.; Weber, W. A.; Stickeler, E.; Meyer, P. T. Gastrin-Releasing Peptide Receptor Imaging in Breast Cancer Using the Receptor Antagonist 68 Ga-RM2 And PET. *Theranostics* **2016**, *6* (10), 1641–1650. https://doi.org/10.7150/thno.14958.

(39) Reubi, J. C.; Maecke, H. R. Approaches to Multireceptor Targeting: Hybrid Radioligands, Radioligand Cocktails, and Sequential Radioligand Applications. *J. Nucl. Med.* **2017**, *58* (Suppl 2), 10S-16S. https://doi.org/10.2967/jnumed.116.186882.

(40) Liolios, C.; Sachpekidis, C.; Schäfer, M.; Kopka, K. Bispecific Radioligands Targeting Prostate-Specific Membrane Antigen and Gastrin-Releasing Peptide Receptors on the Surface of Prostate Cancer Cells. *J. Label. Compd. Radiopharm.* **2019**, *62* (8), 510–522. https://doi.org/10.1002/jlcr.3749.

(41) Handl, H. L.; Vagner, J.; Han, H.; Mash, E.; Hruby, V. J.; Gillies, R. J. Hitting Multiple Targets with Multimeric Ligands. *Expert Opin. Ther. Targets* **2004**, *8* (6), 565–586. https://doi.org/10.1517/14728222.8.6.565.

(42) Eder, M.; Schäfer, M.; Bauder-Wüst, U.; Haberkorn, U.; Eisenhut, M.; Kopka, K. Preclinical Evaluation of a Bispecific Low-Molecular Heterodimer Targeting Both PSMA and GRPR for Improved PET Imaging and Therapy of Prostate Cancer. *Prostate* **2014**, *74* (6), 659–668. https://doi.org/10.1002/pros.22784.

(43) Liolios, C.; Schäfer, M.; Haberkorn, U.; Eder, M.; Kopka, K. Novel Bispecific PSMA/GRPr Targeting Radioligands with Optimized Pharmacokinetics for Improved PET Imaging of Prostate Cancer. *Bioconjug. Chem.* **2016**, *27* (3), 737–751. https://doi.org/10.1021/acs.bioconjchem.5b00687.

(44) Mitran, B.; Varasteh, Z.; Abouzayed, A.; Rinne, S. S.; Puuvuori, E.; De Rosa, M.; Larhed, M.; Tolmachev, V.; Orlova, A.; Rosenström, U. Bispecific GRPR-Antagonistic Anti-PSMA/GRPR Heterodimer for PET and SPECT Diagnostic Imaging of Prostate Cancer. *Cancers (Basel).* **2019**, *11* (9), 1371. https://doi.org/10.3390/cancers11091371.

(45) Lundmark, F.; Abouzayed, A.; Mitran, B.; Rinne, S. S.; Varasteh, Z.; Larhed, M.; Tolmachev, V.; Rosenström, U.; Orlova, A. Heterodimeric Radiotracer Targeting PSMA and GRPR for Imaging of Prostate Cancer—Optimization of the Affinity towards PSMA by Linker Modification in Murine Model. *Pharmaceutics* **2020**, *12* (7), 1–15. https://doi.org/10.3390/pharmaceutics12070614.

(46) Mendoza-Figueroa, M. J.; Escudero-Castellanos, A.; Ramirez-Nava, G. J.; Ocampo-García, B. E.; Santos-Cuevas, C. L.; Ferro-Flores, G.; Pedraza-Lopez, M.; Avila-Rodriguez, M. A. Preparation and Preclinical Evaluation of 68Ga-IPSMA-BN as a Potential Heterodimeric Radiotracer for PET-Imaging of Prostate Cancer. *J. Radioanal. Nucl. Chem.* **2018**, *318* (3), 2097–2105. https://doi.org/10.1007/s10967-018-6285-3.

(47) Bandari, R. P.; Carmack, T. L.; Malhotra, A.; Watkinson, L.; Fergason Cantrell, E. A.; Lewis, M. R.; Smith, C. J. Development of Heterobivalent Theranostic Probes Having High Affinity/Selectivity for the GRPR/PSMA. *J. Med. Chem.* **2021**, *64* (4), 2151–2166. https://doi.org/10.1021/acs.jmedchem.0c01785.

(48) Yan, Y.; Chen, X. Peptide Heterodimers for Molecular Imaging. *Amino Acids* **2011**, *41*, 1081–1092. https://doi.org/10.1007/s00726-010-0546-y.

(49) Abouzayed, A.; Yim, C. Bin; Mitran, B.; Rinne, S. S.; Tolmachev, V.; Larhed, M.; Orlova, A.; Orlova, A. Synthesis and Preclinical Evaluation of Radio-Iodinated GRPR/PSMA Bispecific Heterodimers for the Theranostics Application in Prostate Cancer. *Pharmaceutics* **2019**, *11* (7). https://doi.org/10.3390/pharmaceutics11070358.

(50) Kubas, H.; Schäfer, M.; Bauder-Wüst, U.; Eder, M.; Oltmanns, D.; Haberkorn, U.; Mier, W.; Eisenhut, M. Multivalent Cyclic RGD Ligands: Influence of Linker Lengths on Receptor Binding. *Nucl. Med. Biol.* **2010**, *37* (8), 885–891. https://doi.org/10.1016/j.nucmedbio.2010.06.005.

(51) Liolios, C.; Buchmuller, B.; Bauder-Wüst, U.; Schäfer, M.; Leotta, K.; Haberkorn, U.; Eder, M.; Kopka, K. Monomeric and Dimeric ^{68} Ga-Labeled Bombesin Analogues for Positron Emission Tomography (PET) Imaging of Tumors Expressing Gastrin-Releasing Peptide Receptors (GRPrs). *J. Med. Chem.* **2018**, *61* (5), 2062–2074. https://doi.org/10.1021/acs.jmedchem.7b01856.

(52) Liolios, C.; Patsis, C.; Lambrinidis, G.; Tzortzini, E.; Roscher, M.; Bauder-Wüst, U.; Kolocouris, A.; Kopka, K. Investigation of Tumor Cells and Receptor-Ligand Simulation Models for the Development of PET Imaging Probes Targeting PSMA and GRPR and a Possible Crosstalk between the Two Receptors. *Mol. Pharm.* **2022**. https://doi.org/10.1021/acs.molpharmaceut.2c00070.

(53) Marusyk, A.; Polyak, K. Tumor Heterogeneity: Causes and Consequences. *Biochim. Biophys. Acta - Rev. Cancer* **2010**, *1805* (1), 105–117. https://doi.org/10.1016/j.bbcan.2009.11.002.

(54) Ciccarese, C.; Massari, F.; Iacovelli, R.; Fiorentino, M.; Montironi, R.; Di Nunno, V.; Giunchi, F.; Brunelli, M.; Tortora, G. Prostate Cancer Heterogeneity: Discovering Novel Molecular Targets for Therapy. *Cancer Treat. Rev.* **2017**, *54*, 68–73. https://doi.org/10.1016/j.ctrv.2017.02.001.

(55) Rybalov, M.; Ananias, H. J. K.; Hoving, H. D.; van der Poel, H. G.; Rosati, S.; de Jong, I. J. PSMA, EpCAM, VEGF and GRPR as Imaging Targets in Locally Recurrent Prostate Cancer after Radiotherapy. *Int. J. Mol. Sci.* **2014**, *15* (4), 6046–6061. https://doi.org/10.3390/ijms15046046.

(56) Liolios, C. C.; Fragogeorgi, E. A.; Zikos, C.; Loudos, G.; Xanthopoulos, S.; Bouziotis, P.; Paravatou-Petsotas, M.; Livaniou, E.; Varvarigou, A. D.; Sivolapenko, G. B. Structural Modifications of ^{99m}Tc-Labelled Bombesin-like Peptides for Optimizing Pharmacokinetics in Prostate Tumor Targeting. *Int. J. Pharm.* **2012**, *430* (1–2). https://doi.org/10.1016/j.ijpharm.2012.02.049.

(57) Cheng, C.; Pan, L.; Dimitrakopoulou-Strauss, A.; Schäfer, M.; Wängler, C.; Wängler, B.; Haberkorn, U.; Strauss, L. G. Comparison between 68Ga-Bombesin (68Ga-BZH3) and the CRGD Tetramer 68Ga-RGD4 Studies in an Experimental Nude Rat Model with a Neuroendocrine Pancreatic Tumor Cell Line. *EJNMMI Res.* **2011**, *1*, 34. https://doi.org/10.1186/2191-219X-1-34.

(58) Strauss, L. G.; Koczan, D.; Seiz, M.; Tuettenberg, J.; Schmieder, K.; Pan, L.; Cheng, C.; Dimitrakopoulou-Strauss, A. Correlation of the Ga-68-Bombesin Analog Ga-68-BZH3 with Receptors Expression in Gliomas as Measured by Quantitative Dynamic Positron Emission Tomography (DPET) and Gene Arrays. *Mol. Imaging Biol.* **2012**, *14* (3), 376–383. https://doi.org/10.1007/s11307-011-0508-0.

(59) Escudero-Castellanos, A.; Ocampo-García, B.; Ferro-Flores, G.; Santos-Cuevas, C.; Morales-Ávila, E.; Luna-Gutiérrez, M.; Isaac-Olivé, K. Synthesis and Preclinical Evaluation of the 177 Lu-DOTA-PSMA(Inhibitor)-Lys 3 -Bombesin Heterodimer Designed as a Radiotheranostic Probe for Prostate Cancer. *Nucl. Med. Commun.* **2019**, *40* (3), 278–286. https://doi.org/10.1097/MNM.0000000000000966.

(60) Santos-Cuevas, C.; Ferro-Flores, G.; García-Pérez, F. O.; Jiménez-Mancilla, N.; Ramírez-Nava, G.; Ocampo-García, B.; Luna-Gutiérrez, M.; Azorín-Vega, E.; Davanzo, J.; Soldevilla-Gallardo, I. 177 Lu-DOTA-HYNIC-Lys(Nal)-Urea-Glu: Biokinetics, Dosimetry, and Evaluation in Patients with Advanced Prostate Cancer. *Contrast Media Mol. Imaging* **2018**, *2018*, 1–10. https://doi.org/10.1155/2018/5247153.

(61) Eder, M.; Schäfer, M.; Bauder-Wüst, U.; Hull, W.-E.; Wängler, C.; Mier, W.; Haberkorn, U.; Eisenhut, M. (68)Ga-Complex Lipophilicity and the Targeting Property of a Urea-Based PSMA Inhibitor for PET Imaging. *Bioconjug. Chem.* **2012**, *23* (4), 688–697. https://doi.org/10.1021/bc200279b.

(62) Eder, M.; Neels, O.; Müller, M.; Bauder-Wüst, U.; Remde, Y.; Schäfer, M.; Hennrich, U.; Eisenhut, M.; Afshar-Oromieh, A.; Haberkorn, U.; Kopka, K. Novel Preclinical and Radiopharmaceutical Aspects of [68Ga]Ga-PSMA-HBED-CC: A New PET Tracer for Imaging of Prostate Cancer. *Pharmaceuticals (Basel).* **2014**, *7* (7), 779–796. https://doi.org/10.3390/ph7070779.

Schemes and figures

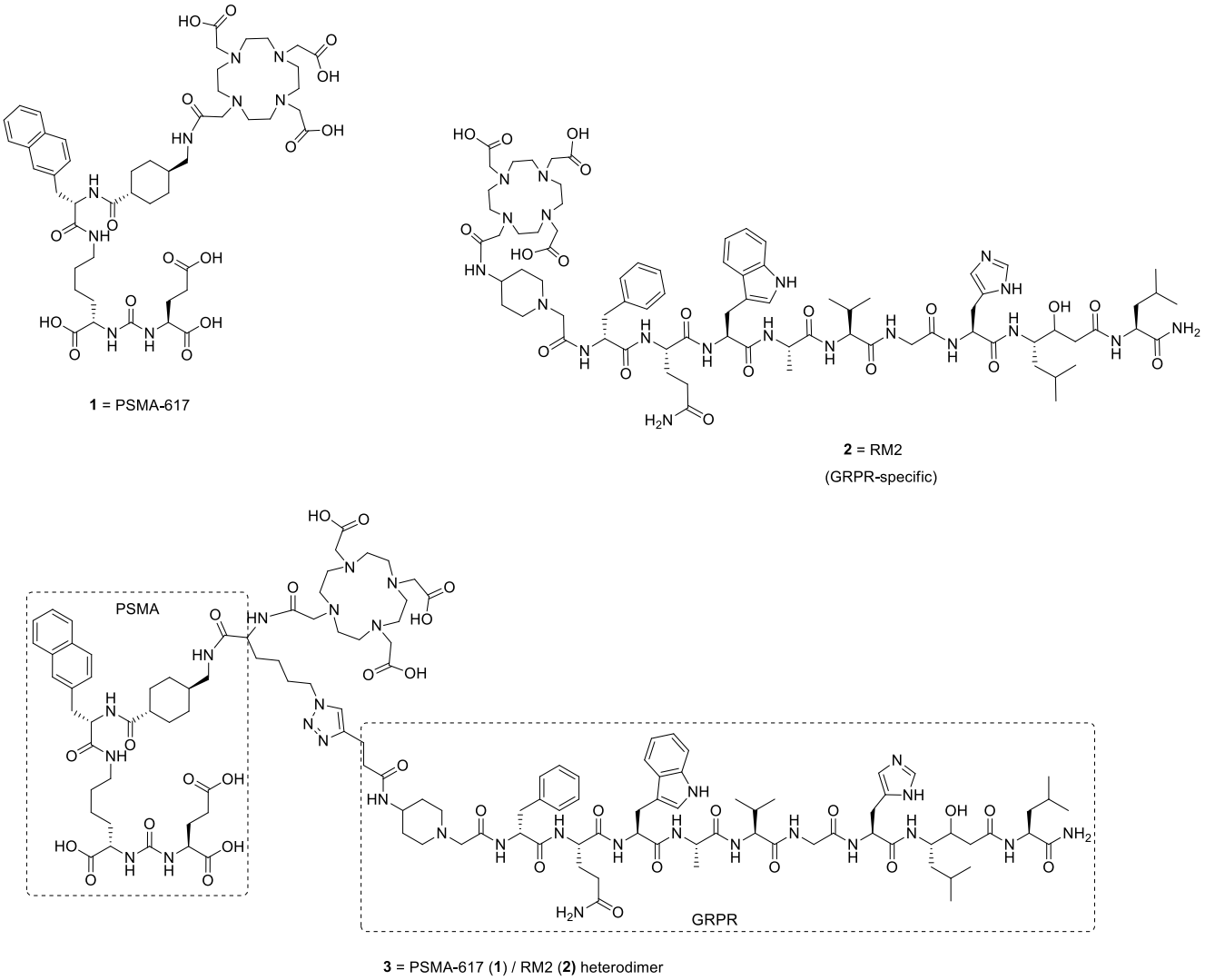

Scheme 1. Chemical structures of PSMA-617 (**1**), RM2 (**2**) and heterodimer **3** of PSMA specific pharmacophore **1** and GRPR specific pharmacophore **2**.

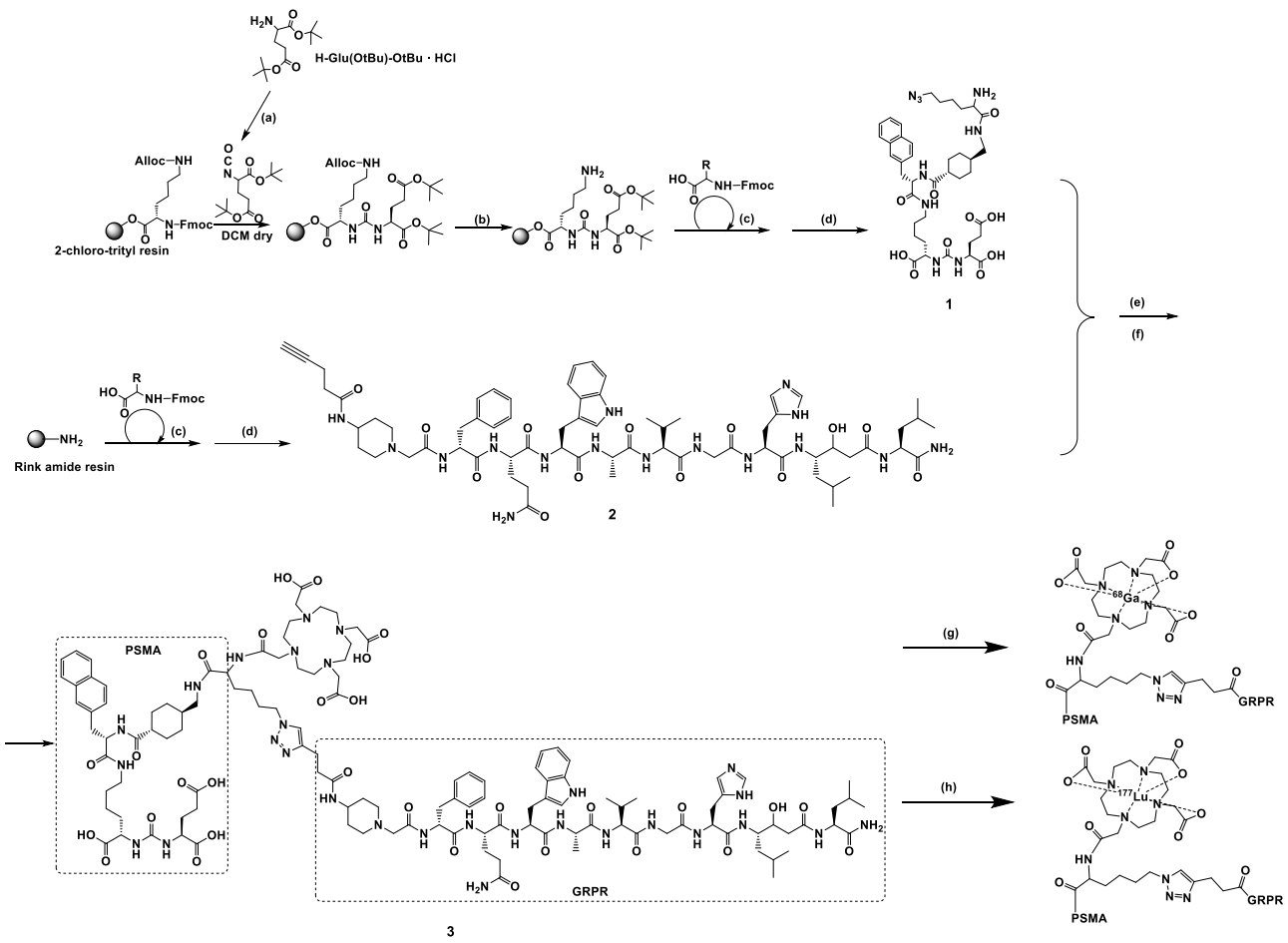

Scheme 2. Chemical synthesis of PSMA specific **4**, GRPR specific **5** and of the heterodimeric conjugate **3**; (a) triphosgene, DIPEA, DCM (°C), (b) $Pd(PPh_3)_4$, morpholine, DCM (dry), (c) amino acid (a.a.) and amino acid derivatives (6-Azido-L-lysine, 4-pentynoic acid) coupling: a.a. , DIPEA, DIC, HBTU, Fmoc deprotection: 40% piperidine in DMF, (d) cleavage mixture: TFA/TIPS/H_2O 95:2.5:2.5 (v/v/v), (e) CuAAC reaction (4 equiv. $CuSO_4$, 4 equiv. Na-ascorbate), (f) DOTA-NHS, EDC, PBS (pH = 8.5), (g) [^{68}Ga]Ga, Hepes buffer (0.25 M), pH = 4.0, 95^{O}C , 30 min, (h) [^{177}Lu]$LuCl_3$, Na-Ac buffer (400 nM), pH= 5.0, 98 °C, 25 min.

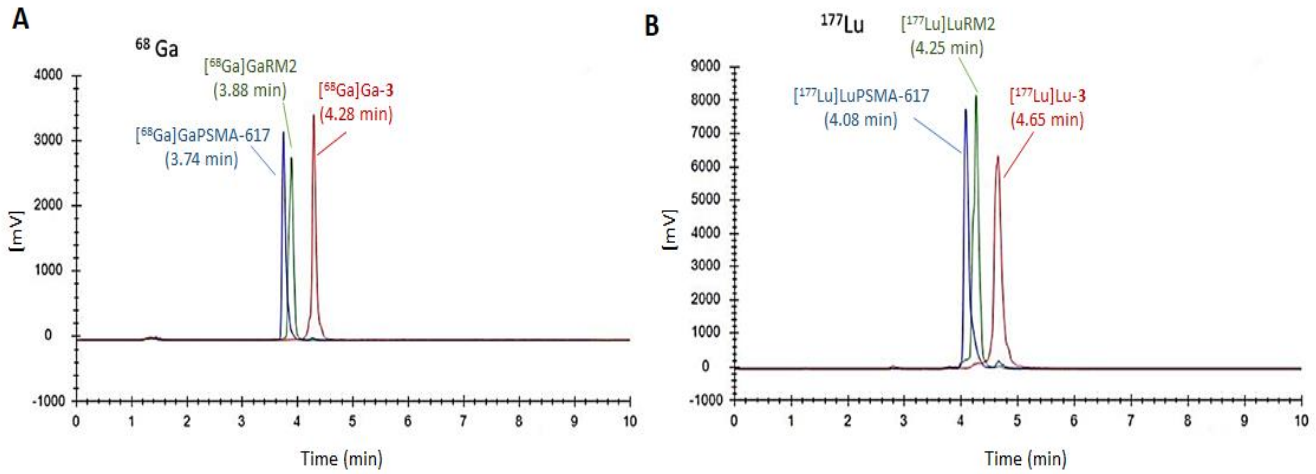

Figure 1. Comparative radio RP-HPLC of (A) [^{68}Ga]Ga-**3** and reference compounds [^{68}Ga]Ga-PSMA-617, [^{68}Ga]Ga-RM2 and (B) [^{177}Lu]Lu-**3** and [^{177}Lu]Lu-PSMA-617, [^{177}Lu]Lu-RM2.

A

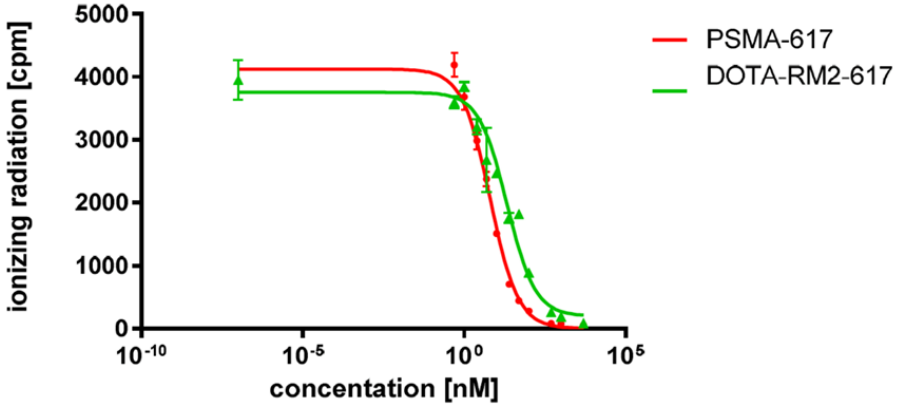

B

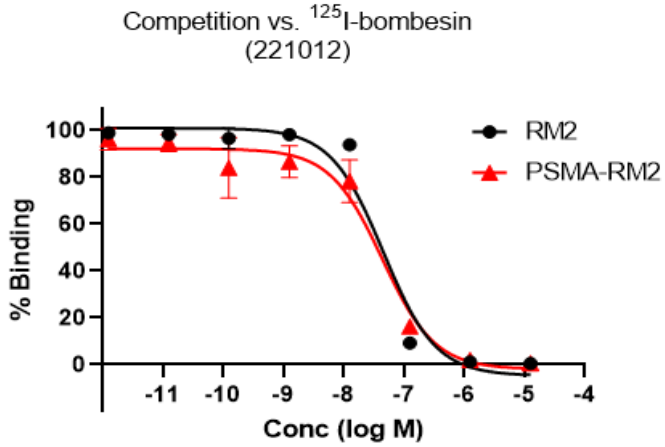

Figure 2 Competitive binding curves plotted using various concentrations (C = 0-5000 nM) of **3** and (A) control PSMA-617 (**1**) against ^{68}Ga-PSMA-10 (standard), (b) control RM2 (**2**) against ^{125}I-bombesin (standard).

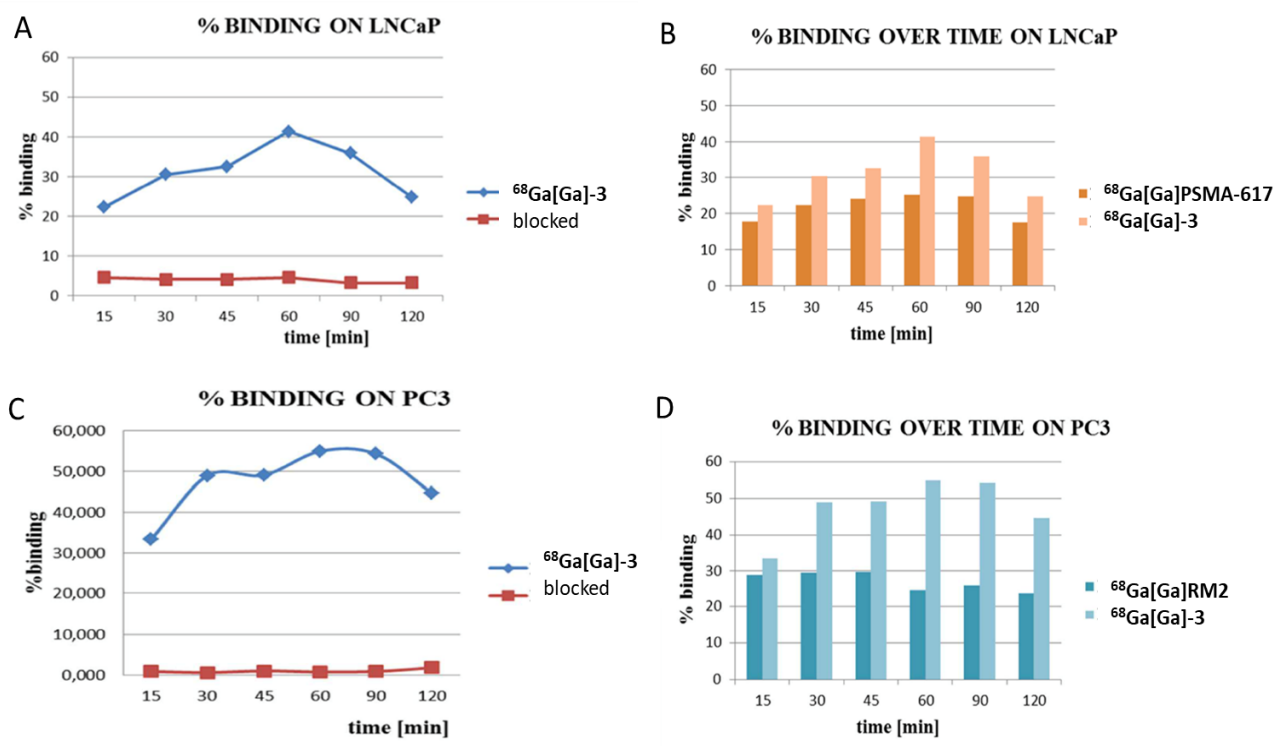

Figure 3 Total cell-bound radioactivity (% of Radioactivity added) over time (0-120 min) of [^{68}Ga]Ga-**3** (30 nM in 1.4 × 10^5 cells) with block (A, C) and with controls [^{68}Ga]Ga-PSMA-617 for LNCaP cells (B) and [^{68}Ga]Ga-RM2 for PC-3 cells (D).

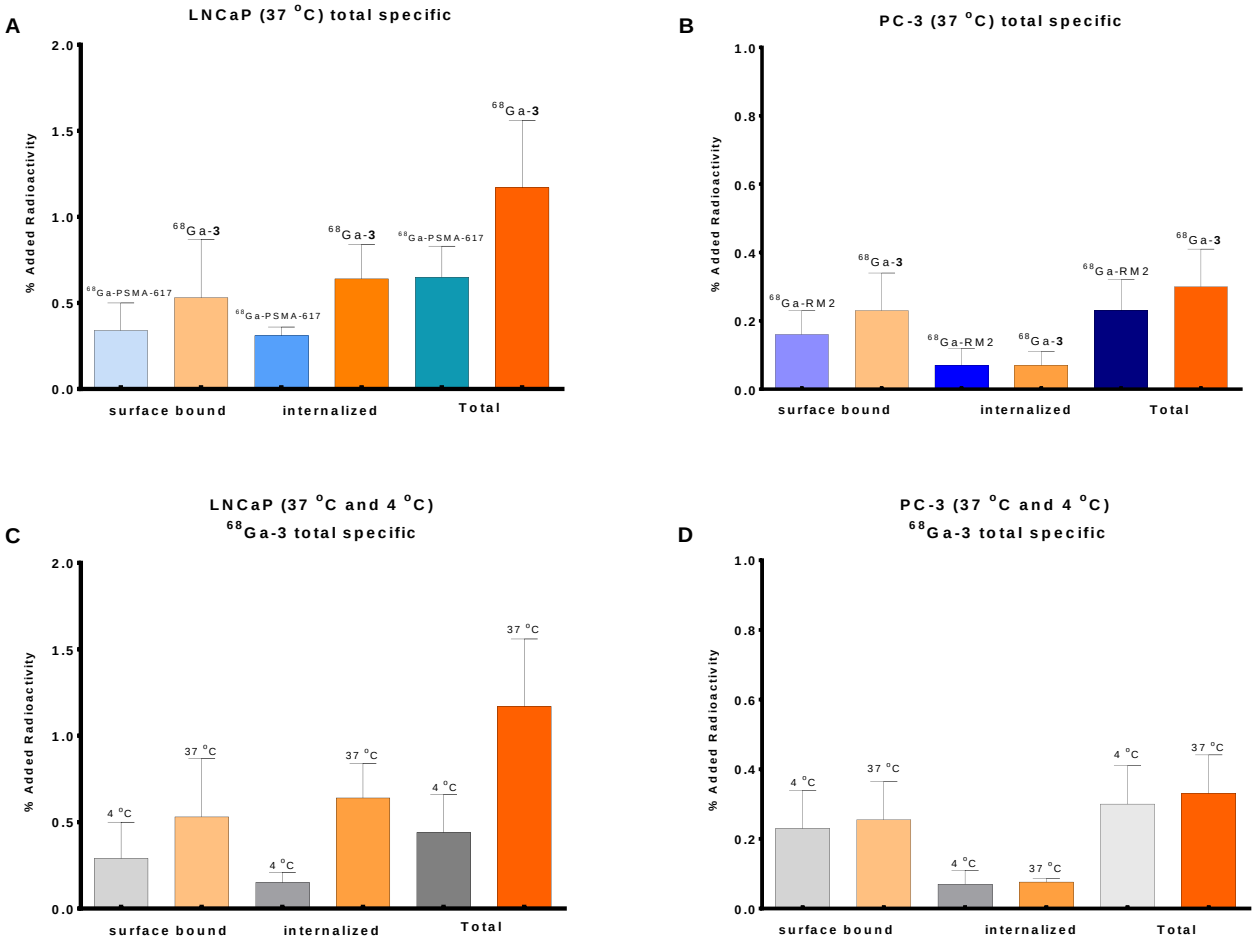

Figure 4. Surface bound, internalized and total cell-bound ligand expressed as % percentage of the added radioactivity in (A), (C) LNCaP and (B), (D) PC-3 cells for [^{68}Ga]Ga-**3** and controls [^{68}Ga]Ga-PSMA-617 and [^{68}Ga]Ga-RM2, at 37 °C and 4 °C.

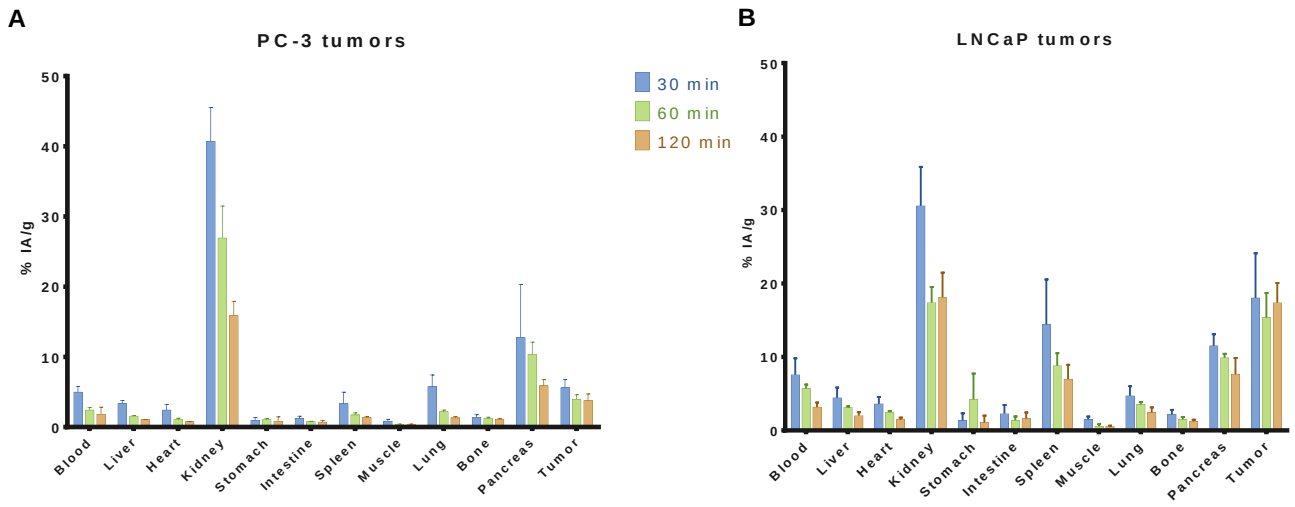

Figure 5. Biodistribution results expressed as % IA/g for [^{68}Ga]Ga-**3** in nude mice bearing PC-3 (A) and LNCaP (B) tumors at three different time points 30, 60 and 120 min p.i.

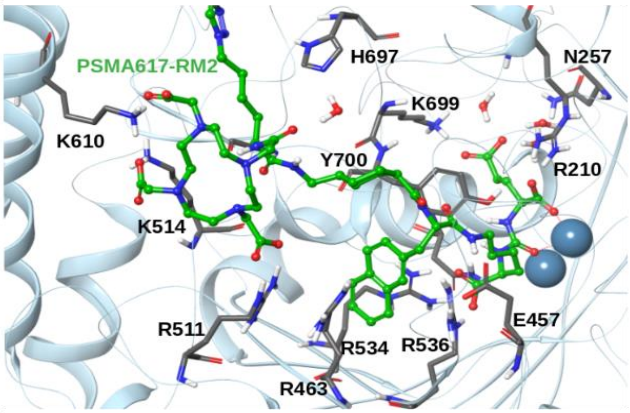

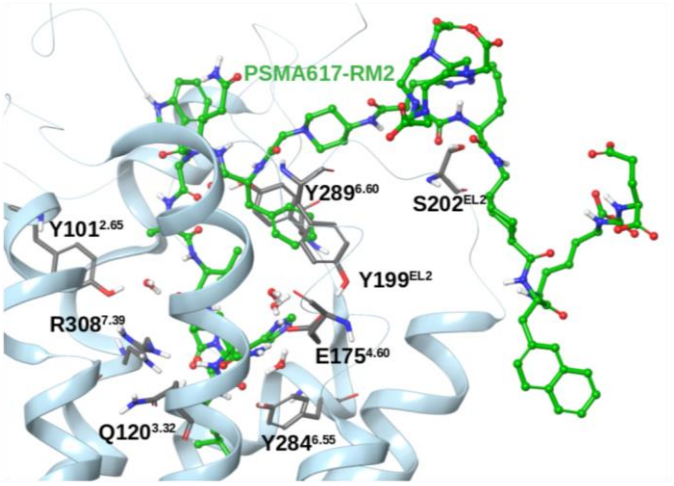

Figure 6. Results from docking calculations of heterodimer **3** (top) inside the PSMA receptor and (bottom) inside the BB2R (ligand's carbons: green, oxygen: red, nitrogen: blue, polar hydrogen: white; receptor is shown with cartoon representation).

Tables

Table 1. MALDI-MS results for compounds **1-3**.

		Calc.M	**$[M+H]^+$**
4	$C_{39}H_{55}N_9O_{10}$	809.92	810.5
5	$C_{67}H_{96}N_{16}O_{13}$	1333.60	1334.4
3	$C_{122}H_{177}N_{29}O_{30}$	2529.93	2530.3

Table 2. Distribution coefficient logD in n-octanol/PBS (pH = 7.4) for [^{177}Lu]Lu-PSMA-617, [^{68}Ga]Ga-RM2, [^{68}Ga]Ga-**3** and [^{177}Lu]Lu-PSMA-617, [^{177}Lu]Lu-RM2, [^{177}Lu]Lu-**3**.

Radionuclide used in the complex	logD [a]		
	PSMA-617 (**1**)	RM2 (**2**)	**3**
[^{68}Ga]Ga	-2.99 ± 0.05	-2.93 ± 0.1	-1.82 ± 0.01
[^{177}Lu]Lu	-3.41 ± 0.50	-3.01 ± 0.08	-2.45 ± 0.01

[a] determined as mean from 3 repeats

Table 3. Binding affinities IC_{50} (nM) or Ki (nM)[$] values of heterodimer **3** and controls PSMA-617 (**1**) and RM2 (**2**) determined against PSMA receptor in LNCaP cells (PSMA+, GRPR-) and GRPR in PC-3 cells (PSMA-, GRPR+).

Compound	LNCaP	PC-3	Ref
3	21.41	43.93	
RM2 (**2**)	-	45.59	
RM2		7.7	[37]
PSMA-617 (**1**)	6.41	-	
PSMA-617	2.34[$]	-	[28]
PSMA-11	12.0 /10.8	-	[61]/[62]
HE_{00}	25.0	9.0	[42]
HE_0	25.4	7.72	[43]
HE_1	17.4	7.28	
HE_2	25.2	4.40	
HE_3	42.4	7.09	
[^{177}Lu]Lu-iPSMA-BN	5.62	3.49	[59]
[^{177}Lu]Lu-PSMA-617	8.69	-	
[^{177}Lu]Lu-BN	-	4.67	
[^{68}Ga]Ga-iPSMA	1.01[$]	-	[46]
[^{68}Ga]GaDOTA-Lys^3-BN	-	48.78[$]	
[^{68}Ga]Ga-iPSMA-BN	4.44	43.69[$]	